ISSN 1023-1935, Russian Journal of Electrochemistry, 2009, Vol. 45, No. 11, pp. 1253–1265. © Pleiades Publishing, Ltd. 2009.
Original Russian Text © Yu.G. Chirkov, V.I. Rostokin, 2009, published in Elektrokhimiya, 2009, Vol. 45, No. 11, pp. 1353–1366.

Fuel Cell with Polymer Electrolyte: Calculation of Overall Characteristics of Oxygen Cathode with Account for Processes of Gas, Vapor, and Heat Exchange

Yu. G. Chirkov[a, z] and V. I. Rostokin[b]

[a]*A.N. Frumkin Institute of Physical Chemistry and Electrochemistry, Russian Academy of Sciences, Moscow, Russia*
[b]*Moscow Engineering Physical Institute, Russia*

Received June 20, 2008; in revised form, December 15, 2008

Abstract—Computer simulation was performed for the processes occurring in the basic elements of the cathode (active layer, gas–diffusion layer) and bipolar plate of a fuel cell with Nafion as electrolyte and a platinum catalyst. Current generation in the active layer was considered together with the heat exchange processes (release of the heat formed in the active layer through the gas–diffusion layer into the bipolar plate), gas and vapor exchange in the gas–diffusion layer and process of the gas reagent (oxygen) saturation by water vapor in the bipolar plate channels. Voltammetric curves and dependences on the cathode potential on the power density, flow dissipated from the active layer to the vapor bipolar plate, actual active layer temperature and reduced partial pressures of oxygen and water vapors near the interface between the active and gas–diffusion layers were calculated. Analysis is performed of the way the heating of the cathode active layer intensifies the process of current generation in it, significantly increasing the value of overall characteristics of the cathode (current and power density).

Key words: fuel cell with Nafion and platinum, oxygen cathode, computer simulation of the process of current generation in the cathode, heating of the cathode active layer, Tafel curves of the cathode, water vapor flow in the direction from the cathode active layer to the bipolar plate, oxygen solubility in Nafion, partial pressure of oxygen at the interface between the active and gas–diffusion layers

DOI: 10.1134/S1023193509110068

INTRODUCTION

In order to provide the operation of a fuel cell with a solid polymer electrolyte (most often, it is Nafion), it is important to provide optimum conditions for operation of a Nafion membrane and active layers of the electrodes and increase protonic conductivity of Nafion in them up to the values of about $\kappa = 1 \times 10^{-1}$ Ohm^{-1} cm^{-1}. The common way to achieve this is humidification of gases supplied into the channels of bipolar plates of the cathode and anode. Herewith, the temperature of saturated vapor in the bipolar plate must be higher than the temperature of the fuel cell operation. It is assumed that the pressure of saturated vapor in the bipolar plate thus becomes higher than the saturated vapor pressure at the interface between the active and gas–diffusion layers and thus a vapor flow is created from the bipolar plate to the active layer, which assists the additional humidification of Nafion and improvement in the fuel cell characteristics.

However, such line of reasoning gives rise to complicated problems. The first of them is the danger of the cathode active layer flooding by water. Indeed, all water flows are directed towards the cathode active layer: water is carried by the flow of protons in the Nafion membrane (from the anode to the cathode); water is evolved as a result of the electrochemical process in the cathode active layer and, finally, water is carried by the water vapor moving, as usually assumed, through the gas–diffusion layer to the same active layer. So, how can a fuel cell function in a steady–state mode under such conditions?

The second problem is heat generation in the cathode active layer. It would seem that it would be primarily dissipated through the gas–diffusion layer into the bipolar plate. But this is prevented by the fact that the active layer temperature coinciding with the fuel cell temperature proves to be below the temperature of saturated vapor in the bipolar plate. So the heat flow turns out to be directed not from the active layer to the bipolar plate but, on the contrary, towards it. Additional active layer heating occurs. Thus, the heat evolved on the cathode can probably be dissipated in a complicated way only through the Nafion membrane and the anode.

We assumed in this reasoning that the cathode active layer temperature coincides with the temperature, at which the fuel cell operates. Let us now abandon this supposition and assume that its heating occurs due to heat evolution on the cathode. Then the cathode active layer temperature can prove to be higher than the tem-

[z] Corresponding author: olga.nedelina@gmail.com (Yu.G. Chirkov).

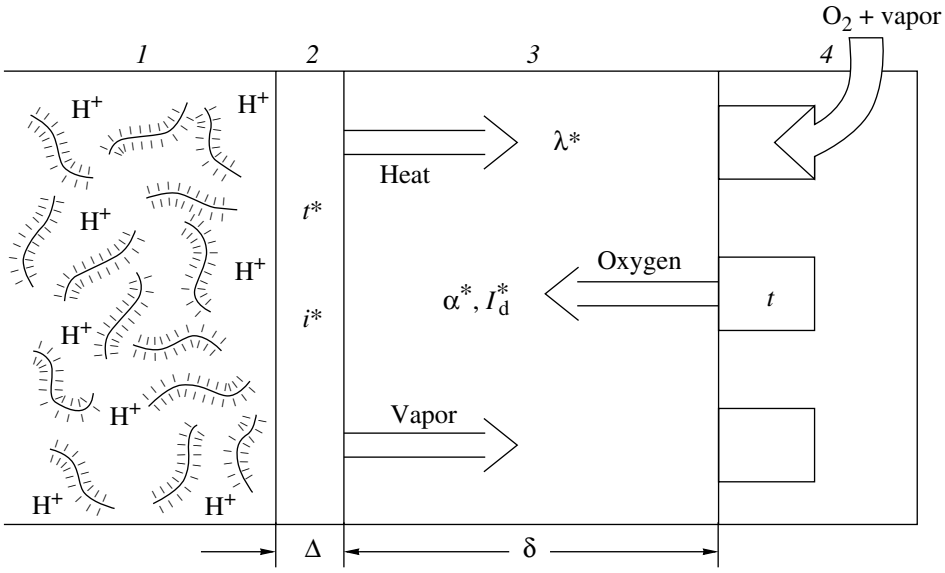

Fig. 1. Schematic drawing of the cathode of a fuel cell with solid polymer electrolyte. (*1*) Nafion membrane, (*2*) active layer, (*3*) gas–diffusion layer, (*4*) bipolar plate.

perature of the saturated water vapor in the bipolar plate channels. In this case, the water vapor flow will be directed from the active layer to the bipolar plate, which can assist eliminating the threat of cathode flooding. Besides, dissipation of excess heat generated on the cathode is facilitated. It can be removed now through the gas–diffusion cathode layer towards the bipolar plate.

This more natural situation will be the subject matter of the present paper.

Fig. 1 presents a schematic image of the cathode of a fuel cell with solid polymer electrolyte in contact with a Nafion membrane and bipolar plate.

An electrochemical reaction of oxygen reduction occurs in the active layer:

$$O_2 + 4H^+ + 4e = 2H_2O. \quad (1)$$

Effectiveness of the cathode operation depends on many factors: on the structure perfection and active layer composition, on its thickness Δ, on the parameters characterizing the gas–diffusion layer, on outer parameters (gas pressure in the bipolar plate channels p^*, degree of oxygen saturation by water). However, the governing factor is the active layer temperature t^*. It affects the value of the key process parameter: the characteristic bulk current density i^*. The rate of process (1) also depends significantly on the effectiveness of molecular oxygen supply towards the active layer (Fig. 1), on the value of the thus arising outer–diffusion limitations, on the degree of effectiveness of the process of gas and vapor exchange in the gas–diffusion layer. Here, the following parameters are of importance: I_d^* is the characteristic diffusion current in the gas–diffusion layer and α^* is the ratio of the characteristic rate of the vapor–gas mixture filtration to its diffusion rate. The same parameters determine the effectiveness of the process of removal of water formed in the cathode active layer. The vapor flow (Fig. 1) is directed from the active layer to the bipolar plate because, as shown further, the active layer temperature t^* causes an increase in the gas temperature t in the bipolar plate.

Let us use the following assumptions. If dry gas (oxygen or hydrogen) is supplied to the bipolar plate, then temperature t is equal to the temperature, at which the fuel cell operates. But if a gas saturated by water vapor is supplied into the bipolar plate, then temperature t becomes equal to the saturated vapor temperature. Let us assume further than $t^* > t$: heat is evolved in the active layer of the fuel cell cathode and it must be dissipated. It is natural to assume that the heat flow (Fig. 1) is directed towards the bipolar plate. Effectiveness of heat dissipation must be determined by the value of thermal conductivity of the gas–diffusion layer λ^* and its thickness δ.

The process of current generation in the active layer and the corresponding processes of gas, vapor, and heat exchange are undoubtedly closely related. Let us proceed to the analysis of the character of this relationship.

CONSIDERATION OF HEAT EXCHANGE

Fuel cells with Nafion as electrolyte and a platinum catalyst feature very high overall characteristics (their power density exceeds 1 W/cm^2). The amount of heat evolved in the fuel cells also increases simultaneously with an increase in the power.

Heating of the cathode active mass results inevitably in an increase in the exchange current. In [1], the dependence of exchange current i_0 on the temperature

in the case of the oxygen reduction process on platinum is presented as follows:

$$i_0 = i_0^{\text{ref}} \exp\{8804[1/(50 + 273) - 1/(t + 273)]\}, \quad (2)$$

where t is given in centigrade. Let us assume that the exchange current for platinum at temperature $t = 50°C$ in the range of high potentials $i_0^{\text{ref}} = 10^{-8}$ A/cm^2 [2]. Then, as shown by estimations, the exchange current density increases by 5 orders of magnitude at an increase in the temperature in the range from 20 to 200°C. Thus, heating of the cathode active layer, its operation at increased temperatures can also significantly affect the value of the characteristic bulk current determined by the expression:

$$i^* = i_0 S, \quad (3)$$

where S is the active fraction of the catalyst specific surface area in the cathode active layer. And this, in its turn, must result in a significant increase in the value of the cathode overall current I.

If the thermal conductivity of the gas–diffusion layer is insufficiently high to dissipate efficiently the heat formed in the active layer, the active layer temperature must inevitably grow further at an increase in the current generated on the cathode, which would cause an additional increase in the overall current. This process would occur until the temperature of the active layer reaches a certain equilibrium value t^*, at which the amount of heat evolved on the cathode becomes equal to the amount of heat dissipated through the gas–diffusion layer. This established heat flow is obviously proportional to the difference of temperatures $(t^* - t)$, where t is the gas temperature in the bipolar plate (Fig. 1).

To estimate the degree of the cathode active layer heating and its effect on the value of the overall characteristics of the cathode, we make a number of assumptions facilitating the calculations.

(1) Let us assume that the heat exchange between the membrane and active layer is absent and the dissipation of the heat evolved in the cathode active layer occurs entirely in the direction of the gas–diffusion layer. Such an assumption does not seem forced. The calculations of distribution of heat flows in the fuel cell with Nafion were carried out in a number of works [3–5]. It is shown that if the degree of gas humidification by the saturated vapor on the anode and cathode is approximately similar, the temperature profile in the fuel cell looks like an equilateral trapezium; herewith, the heat flow in the Nafion membrane can be assumed negligibly low. Thus, if certain not too awkward conditions are observed, a remarkable option of studying the cathode heat exchange as "isolated" from the other fuel cell parts appears.

(2) As the active layer thickness (tens and even several μm) is much lower than the thickness of the gas–diffusion layer (hundreds of μm), let us assume in the calculations that the equilibrium temperature through the active layer is constant and is equal to t^*.

(3) Let us assume the thermophysical properties of the gas–diffusion layer constant across the layer, so that heat transmission in it will be characterized by the thickness of the gas–diffusion layer and effective thermal conductivity independent of the coordinates.

(4) To prevent the excessive sophistication of calculations, let us assume the performance of the current generation process in the cathode constant and independent of the value of the cathode potential.

Then the condition of equality of the flows of heat generated in the cathode active layer and heat dissipated will be presented as follows:

$$(1 - \eta)I(\Delta, t^*)E = \lambda^*(t^* - t)/100\delta. \quad (4)$$

In this equality, η is the performance of the current generation process in the fuel cell, $I(\Delta, t^*)$ is the overall current of the cathode (its value depends on the active layer thickness Δ and on the value of equilibrium temperature t^*), E is the cathode potential, λ^* is the effective thermal conductivity of the gas–diffusion layer, δ is the thickness of the gas–diffusion layer.

The simplest analysis of equality (4) shows the following. Let us consider the limiting variants. If the effective thermal conductivity of the gas–diffusion layer is infinitely high, i.e., $\lambda^* = \infty$, then the condition of $t^* - t = 0$ must be fulfilled due to the finiteness of the product of the quantities in the leftmost part of equation (4). Thus, the heating of the cathode active layer is fully absent and the heat evolved in the active layer is freely dissipated through the gas–diffusion layer. Another limiting case consists in parameter λ^* tending to zero. Then, obviously, the active layer temperature t^* must tend to ∞. The gas diffusion layer fails the task of heat dissipation; a significant active layer heating occurs resulting in very high temperatures t^* and anomalously high overall current values.

CONSIDERATION OF GAS AND VAPOR EXCHANGE

The main parameters determining rates and regularities of the gas and vapor exchange processes in the gas diffusion layer are the diffusion current I_d [6]

$$I_d = I_d^* \varepsilon, \quad (5)$$

where I_d^* is the characteristic diffusion current in the gas–diffusion layer, factor $\varepsilon = p^*/p_0^*$, p^* is the gas pressure in the bipolar plate channels, $p_0^* = 101$ kPa, and parameter α

$$\alpha = \alpha^*\varepsilon, \quad (6)$$

where α^* is the ratio of the characteristic rate of the vapor–gas mixture filtration to its diffusion rate It is convenient to present parameter α, same as I_d, as two cofactors: the structural one determined by the properties of the gas–diffusion layer (factors α^* and I_d^*) and

Table 1. Dependence of the pressure of saturated water vapors on the temperature

t, °C	P_w, kPa
20	2.84
50	13.3
80	48.2
115	168
140	360
160	622
200	1615

barometric one depending on the value of the general pressure in the bipolar plate channels p^* (factor ε).

Statement of the problem regarding the gas and vapor exchange in the gas–diffusion layer also requires setting the values of the gas partial pressure values (oxygen and nitrogen in the case of an air cathode) and the pair at the interfaces of the gas–diffusion layer.

At the interface with the gas–diffusion layer with a bipolar plate (Fig. 1):

$$y = 0, p = p_0, p_N = p_{N0}, p_w = p_{w0}, \quad (7)$$

where p_0, p_{N0}, p_{w0} are the values of reduced (divided by p^*) partial pressure of oxygen, nitrogen, and water vapor.

At the interface between the active layer and the gas–diffusion layer:

$$y = \delta, p = p_s, p_N = p_n, p_w = p_{w1}, \quad (8)$$

where p_s, p_n, p_{w1} are the reduced partial pressures of oxygen, nitrogen, and water vapors (the coordinate axis is directed from the bipolar plate towards the active layer, so that the oxygen flow in Fig. 1 is positive and the vapor flow is negative).

Of the six values in (7) and (8), three are the set task options. The fact is that the pressure of the saturated vapor pressure in the bipolar plate channels P_w can be determined using the following formula:

$$P_w = 101\exp\{4885\,[1/(100 + 273) - 1/(t + 273)]\}, \quad (9)$$

where t is given in centigrade. The values of the saturated vapor pressure P_w calculated according to formula (9) at the temperatures in the range from 20 to 200°C are presented in Table 1. Pressure P_w varies in a wide range at an increase in the temperature: from several units to more than 1600 Pa.

Knowing P_w, one can also estimate the value of reduced partial vapor pressure at the interface between the gas–diffusion layer and bipolar plate p_{w0}. Namely,

$$p_{w0} = P_{w0}/p^*. \quad (10)$$

In its turn, the knowledge of p_{w0} allows determining reduced partial pressure values of the gases in the bipolar plate channels. Obviously, in the case of an oxygen cathode (in this case, the p_{N0} and p_n values in (7) and (8) must be assumed strictly equal to zero):

$$p_0 = 1 - p_{w0}, \quad (11)$$

in the case of an air cathode:

$$p_0 = 4(1 - p_{w0})/5, \quad (12)$$

$$p_{N0} = (1 - p_{w0})/5. \quad (13)$$

The other three quantities (of the six above listed), p_{w0}, p_s, and p_n, are not initially known and must be determined in the course of calculating the partial pressure distribution through the gas–diffusion layer and correlation of the solutions for the p, p_N, p_w functions with the solutions for the functions characterizing the cathode active layer.

The method of calculating the cathode overall characteristics with account for the processes of gas and vapor exchange in the gas–diffusion layer is described in [7]. As shown in this paper, the values of the reduced overall current at the cathode $\bar{I} = I/I_d$, reduced flow of water vapors $\overline{I_w} = nFI_w/I_d$, and reduced partial pressure of nitrogen at the active layer surface p_n at the interface with the gas–diffusion layer are fully determined by the set of the following equations:

$$\bar{I} = \alpha^2\{[1 - (\Sigma_1)^2]/2\}[p_0\exp\alpha - p_s\exp(\alpha\Sigma_1)]/[(\alpha - 1)\exp\alpha - (\alpha\Sigma_1 - 1)\exp(\alpha\Sigma_1)], \quad (14)$$

$$\overline{I_w} = \alpha^2\{[1 - (\Sigma_1)^2]/2\} \times [p_{w0}\exp\alpha - p_{w1}\exp(\alpha\Sigma_1)]/[(\alpha - 1)\exp\alpha - (\alpha\Sigma_1 - 1)\exp(\alpha\Sigma_1)], \quad (15)$$

$$p_n = p_{N0}\exp[\alpha(1 - \Sigma_1)]. \quad (16)$$

Expressions (14)–(16) include the Σ_1 quantity. It is equal to the sum of all the reduced partial pressures at the interface separating the active layer from the gas–diffusion layer, namely: $\Sigma_1 = p_s + p_n + p_{w1}$.

It remains to point out how one can find another parameter required in the calculations: the reduced partial pressure of oxygen at the active layer/gas–diffusion layer interface p_s. This value is determined according to the condition of joining the solutions obtained for the active and gas–diffusion layers. The current generated in the active layer must be equal to the outer–diffusion

current (the flow of oxygen molecules in the gas–diffusion layer). It can be shown that the latter condition is equivalent to the following equality:

$$c_s = p_s, \quad (17)$$

where c_s is the solubility of oxygen in Nafion at the interface between the active and gas–diffusion layers depending on the pressure.

PROCEDURE OF CALCULATION OF CATHODE OVERALL CHARACTERISTICS

The procedure of calculation of the overall characteristics of the cathode includes the following stages.

First of all, one must decide if the dry or humidified gas (oxygen or air) is supplied to the bipolar plate channels. If it is dry, temperature t (Fig. 1) coincides with the temperature, at which the fuel cell operates ($t^* = t$) and the reduced partial pressure of water vapors in the bipolar plate channels $p_{w0} = 0$. If the gas is saturated by water vapors, t coincides with the temperature of saturated vapors and the partial pressure of vapors in the channels is calculated according to formula (9) and the values of reduced partial pressures of gases are estimated according to formulas (10)–(13).

Further, providing the value of all parameters characterizing the cathode (Fig. 1)—its potential E, the pressure of the gas–vapor mixture in the bipolar plate channels p^*, the thickness of the active Δ and gas–diffusion δ layers, effective thermal conductivity of the gas–diffusion layer λ^* and also parameters I_d^* and α^*, one can immediately proceed to calculations.

At first, an arbitrary value of the cathode active layer temperature t^* ($t^* > t$) is chosen and the value of the overall current I generated in the cathode active layer is calculated. A special regularity of this calculation consists in the fact that two Tafel curve slopes are observed in the case of oxygen reduction on platinum in acidic media. The way the overall characteristics of the cathode active layer must be calculated is shown in [8].

It will also be noted that the calculated current is a function not only of temperature, but also of the solubility of oxygen in Nafion at the interface between the active and gas–diffusion layers $c_s - I(t^*, c_s)$. Thus, the c_s value must also be varied and the method of successive iterations must be used to choose it so that condition (17) will be fulfilled and current $I(t^*, c_s)$ will be equal to the current calculated according to formula (14), in which $I = I(p_s)$.

Having ascertained that equalities $I(t^*, c_s) = I(p_s) = I(t^*)$ are fulfilled, one can proceed to the further calculation procedure. Then the obtained pair of I and t^* values is substituted into equality (4). If the leftmost part of equality (4) is higher than its rightmost part, this means that the gas–diffusion layer does not provide adequate heat dissipation and the arbitrarily chosen t^* value must be changed: increased. Variation of parameter t^* must be performed until the leftmost and rightmost parts of expression (4) become equal. This provides true values of overall current I and cathode active layer temperature t^*.

RESULTS OF CALCULATION OF CATHODE OVERALL CHARACTERISTICS

Let us choose the value of the cathode active layer thickness to be $\Delta = 3$ μm. Assuming that the fuel cell operates at $t = 80$°C, the bulk current density corresponding to this temperature in the range of high potentials $i^* = 1.04 \times 10^{-1}$ A/cm^3. Let us assume further that the gas–diffusion layer is characterized by the further parameters. Its thickness $\delta = 400$ μm, effective thermal conductivity $\lambda^* = 0.1$ W/mK (λ^* was experimentally estimated in [5, 9–11], it was shown that the order of magnitude of λ^* is tenths of W/mK). Details of estimation of values I_d^* and α^* are presented in [6]; let us assume $I_d^* = 1.035$ A/cm^2 and $\alpha^* = 0.156$.

Let us consider the functioning of an oxygen cathode, when oxygen reaches the bipolar plate channels already humidified. Let the temperature of saturated water vapors in the channels $t = 95$°C and the overall pressure of vapor and oxygen be $p^* = 101$ kPa. The results of calculation of key overall characteristics of an oxygen cathode, Tafel E, $\log I$-curves and dependences on potential E of power density W, reduced flow of water vapors in the gas–diffusion layer $\overline{I_w}$, active layer temperature t^* and reduced partial pressures of oxygen p_s and water vapors p_{w1} at the interface between the active and gas–diffusion layers are presented in Fig. 2 and are designated as curves *1*.

Overall current I fast assumes the low limiting value, $I_{lim} = 0.17$ A/cm^2. As parameter α^* is low, the principal role in a gas–diffusion layer is played not by the filtration (in this case, inequality $\alpha^* \geq 1$ must be fulfilled), but by the diffusion flows. Thus, the process of Stefan diffusion occurs. Therefore, the oxygen pressure value in the bipolar plate channels plays a decisive role in the current generation in the cathode active layer.

Vapor pressure $P_{w0} = 84.5$ kPa in the bipolar plate channels, at $\varepsilon = 1$ ($p^* = 101$ kPa, formulas (5), (6)) and $t = 95$°C, according to formula (9). Therefore, the reduced partial pressure of the vapor $p_{w0} = 0.84$. Then it follows from (11), the reduced partial pressure of oxygen in the bipolar plate channels is low, $p_0 = 0.16$ (Fig. 2e, curve *1*). In dry oxygen, obviously, $p_0 = 1.0$. The low value of partial pressure of oxygen in the bipolar plate channels (which is caused by increased oxygen humidification) results in a drastic decrease in the oxygen diffusion flow towards the active layer and therefore in a significant decrease in the limiting value of the cathode overall current (Fig. 2a, curve *1*).

Accordingly, the cathode power density (Fig. 2b, curve *1*), vapor flow (Fig. 2c, curve *1*) decrease, the active layer heating turns out to be low (Fig. 2d, curve *1*)

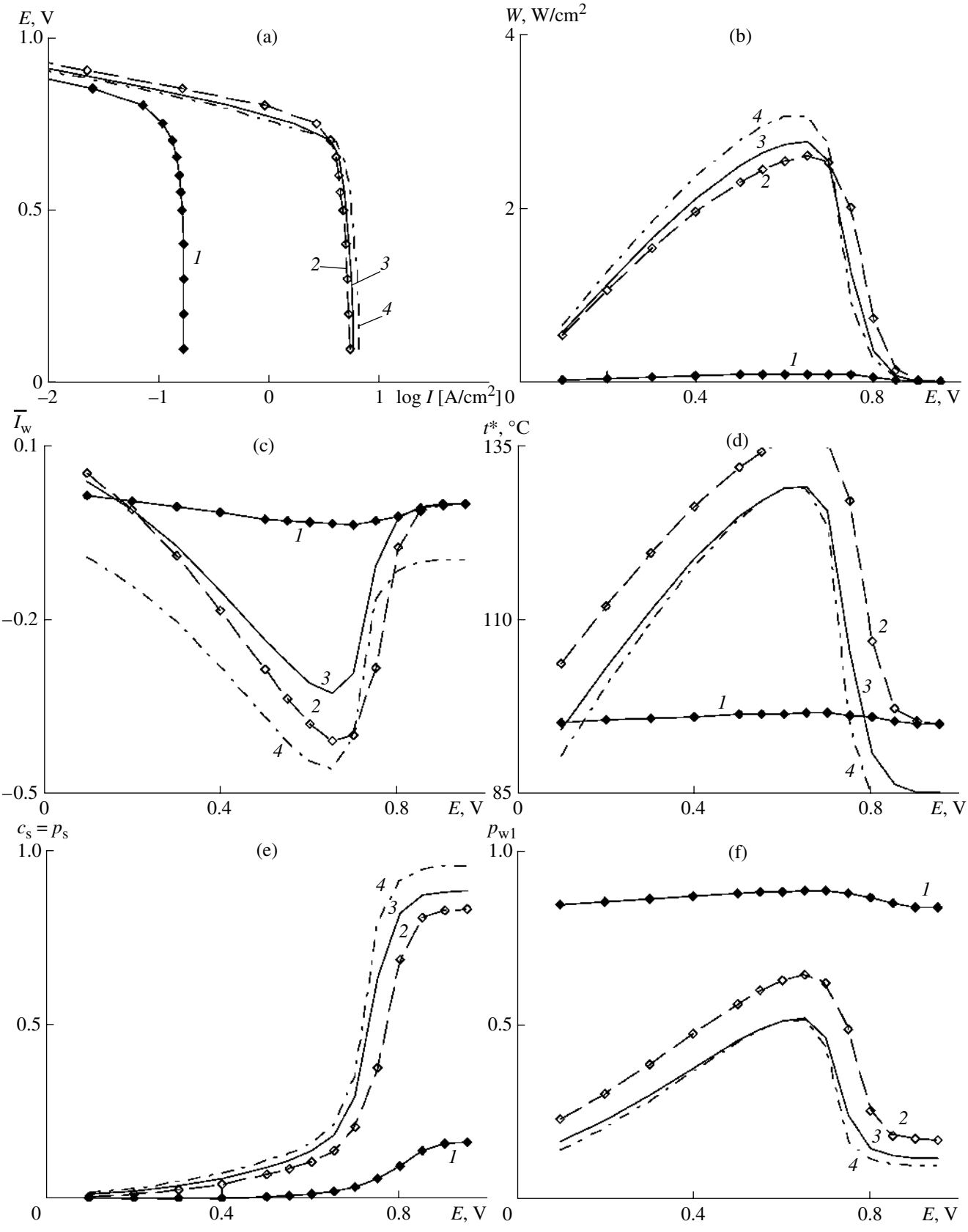
E, V
(a)
1.0
0.5
0
–2
–1
0
1
log I [A/cm2]
1
2
3
4
W, W/cm2
(b)
4
2
0
0.4
0.8
E, V
1
2
3
4
$\overline{I}_w$
(c)
0.1
–0.2
–0.5
0
0.4
0.8
E, V
1
2
3
4
t*, °C
(d)
135
110
85
0
0.4
0.8
E, V
1
2
3
4
$c_s = p_s$
(e)
1.0
0.5
0
0.4
0.8
E, V
1
2
3
4
p_{w1}
(f)
1.0
0.5
0
0.4
0.8
E, V
1
2
3
4

Fig. 2. (a) Tafel curves and dependences on the cathode potential of (b) power density, (c) reduced flow of water vapor, (d) active layer temperature, (e) oxygen solubility in Nafion, and (f) reduced oxygen partial pressure at the interface of the active and gas–diffusion layers. The working fuel cell temperature is 80°C, $i^* = 1.04 \times 10^{-1}$ A/cm^2, $\lambda^* = 0.1$ W/mC, $\delta = 400$ μm, $\Delta = 3$ μm. Curves: (*1*) oxygen, saturated by vapor at $t = 95$°C, $p^* = 101$ kPa; (*2*) oxygen, saturated by vapor at $t = 95$°C, $p^* = 505$ kPa; (*3*) oxygen, saturated by vapor at $t = 85$°C, $p^* = 505$ kPa; (*4*) dry oxygen, $p^* = 505$ kPa.

and the reduced partial pressure of the vapor near the active layer has practically the same value, as in the bipolar plate channels (Fig. 2f, curve *1*).

The negative effect of increased humidity of gases at the inlet to the gas chamber can be significantly decreased due to an increase in the overall pressure of the vapor–gas mixture in the bipolar plate channels. Let $p^* = 505$ kPa, then $\varepsilon = 5$ and according to formulas (9)–(11), the reduced partial pressure of oxygen in the bipolar plate channels reaches now the value of $p_0 = 0.83$ (Fig. 2e, curve *2*), and the reduced partial pressure of the vapor here is only $p_{w0} = 0.17$ (Fig. 2f, curve *2*).

At a fivefold increase in the pressure, the characteristic diffusion current of oxygen also increases by five times. Now, according to formulas (5) and (6), $I_d = 5.175$ A/cm^2 and $\alpha = 0.78$. Accordingly, the limiting value current increases considerably (curves *1* and *2*, Fig. 2a). Low currents result in a negligible cathode active layer heating (curve *1* in Fig. 2d), while high currents cause an increase in temperature t^* at potential $E = 0.65$ V to $t^* = 137$°C (curve *2* in Fig. 2d).

Overall currents fast reaching the limiting values in Fig. 2a (approximately at potential $E = 0.7$ V) is due to the fact that a sudden current increase results in a fast decrease in the reduced partial pressure of oxygen at the interface between the active and gas–diffusion layers (Fig. 2e). Reduced partial pressure of oxygen is already low, $p_s = 0.21$ in curve *2* of this figure at potential $E = 0.7$ V.

Let us now consider two other variants of the values of key parameters. Let the pressure in the bipolar plate channels still be $p^* = 505$ kPa, but in one case, oxygen is saturated by water vapors at $t = 85$°C (curves *3*, Fig. 2) and in the other case oxygen in the bipolar plate channels is dry (curves *4*, Fig. 2).

If one compares curves *3*, *4* in Fig. 2 with curve *2* (they were all obtained at $p^* = 505$ kPa), one can see that the character of variation of overall currents and specific density values with the potential (Fig. 2a and 2b) varies rather slightly. On the other hand, $\overline{I}_w$, E-curves are significantly transformed. In Fig. 2c, all water vapor flows are negative; this means that they are directed from the active layer towards the bipolar plate (Fig. 1). Herewith, the flows turn out to be minimum at the oxygen humidification by saturated vapor at $t = 85$°C (curve *3* in Fig. 2c).

This result correlates well with the recommendations worked out on the basis of the working practice with fuel cells with Nafion as electrolyte and a platinum catalyst. Usually, it is necessary to maintain optimum conditions for its humidification to achieve high conductivity of the solid polymer electrolyte. For this purpose, different approaches were suggested [12]. The most widespread means is saturation of gas reagents in the bipolar plate channels by water vapors. For example, it is recommended in [13] to increase the temperature of the oxygen or air cathode by 5°C (from $t = 80$°C, at which the fuel cell functions) and the temperature of the hydrogen anode by 10°C.

The data of Fig. 2c show that there is the optimum of gas humidification in the bipolar plate channels. Usage of dry (curve *4* in Fig. 2c) or too humidified oxygen (curve *2* in Fig. 2c) results in a water excess loss by the active layer and adjacent Nafion membrane. Here, one should pay attention to the following fundamental circumstance.

Humidification of oxygen or air supplied to the cathode (in the bipolar plate channels) does not result in an additional supply of water (vapor flow) to the active cathode layer, as it could be if the heating of the cathode active layer were absent and its temperature were equal to the temperature of the fuel cell operation.

In practice, the situation is quite different. Significant increase in the cathode active layer temperature occurs. As a result of this, the saturated vapor pressure at the interface of the active and gas–diffusion layers exceeds the vapor pressure in the bipolar plate channels and the vapor flow appears to be directed not to the cathode active layer but away from it, towards the bipolar plate. But this vapor flow is not constant. Transition from dry oxygen to progressively humidified gas (increase in the vaporization temperature in the bipolar plate channels) passes the optimum, i.e., there is a temperature value at which water loss by the membrane and active layers reaches its minimum.

VARIATION OF PRINCIPAL PARAMETERS OF CATHODE

In the case of the discussed phenomena, it is useful to analyze the role of the factors leading to a significant increase in the overall current generated in the cathode active layer.

Naturally, heating of the cathode active layer can occur only in the case of a highly–active catalytic mass if the characteristic bulk current density in the range of high potentials i^* is already sufficiently high. One can show that formula (3) can be rewritten in a more detailed form as follows:

$$i^* = i_0 S = i_0 \eta g_s S^*, \quad (18)$$

where i_0 is the exchange current, g_s is the bulk concentration of the grains of the support (with the catalyst) in the active layer, S^* is the specific surface area of plati-

Table 2. Estimation of the dependence of the characteristic bulk current density in the range of high potentials (the process of oxygen reduction on Pt in the active layer of the cathode with Nafion) on the fuel cell working temperature

t, °C	i^*_{min}, A/cm^3	i^*_{max}, A/cm^3
60	5.06×10^{-5}	5.06×10^{-2}
80	2.3×10^{-4}	2.3×10^{-1}
95	6.44×10^{-4}	6.44×10^{-1}

num per active layer volume unit if it is fully filled by the support grains. Thus, the product of $g_s S^*$ is the specific surface area of platinum per active layer volume unit. A feature of the electrodes with the solid polymer electrolyte consists in the fact that not all of the catalyst can participate in the current generation process. Let us designate the catalyst active surface fraction as η. Then the product of $\eta g_s S^*$ represents the specific surface area of platinum in the active layer that actually participates in the current generation process.

Let us now determine surface area S^*. Usually, it is not this quantity with the dimension of [cm^2/cm^3 = cm^{-1}] present in the theoretical formulas that is determined, but the specific surface area of platinum per platinum mass S^{**}, the quantity with dimension of [m^2/g of Pt]. The expression relating quantities S^* and S^{**} is as follows:

$$S^* = \rho_p S^{**}(1 - \nu)/\{1 + (\rho_p/\rho_c)[(1 - g_w)/g_w]\}, \quad (19)$$

where ρ_p = 21.5 g/cm^3 is the density of platinum, ρ_c = 1.8 g/cm^3 is the density of the support (carbon black), ν is the porosity of the support grains, g_w is the platinum content in the support grains.

Let us find sufficiently approximately, so to speak, the "upper" and "lower" estimates of the S^* value. As shown by the data in the literature, η varies from the values of 60–70 [14] to 75–98% [15, 16]. Naturally, the minimum of this value will be assumed to be η = 50%, the maximum will be η = 100%. If one aims at the optimum structure of the active layer of the cathode with Nafion and platinum [17], then it contains no cavities (g_0 = 0) and the bulk concentration of support grains g_s = 0.525. Let us assume S^{**} = 10 m^2/g of Pt as the minimum S^{**} value and S^{**} = 100 m^2/g of Pt as the maximum S^{**} value. Let us assume that the minimum of the S^* value is provided by the support grain porosity ν = 0.8, while the maximum corresponds to ν = 0.2. Let us choose the minimum platinum content in the support grains to be g_w = 20 wt %, while the maximum is assumed to be g_w = 80 wt %.

Then $S^*_{min} = 8.8 \times 10^3$ cm^{-1}, $S^*_{max} = 4.3 \times 10^6$ cm^{-1}, and $S_{min} = (\eta g_s S^*)_{min} = 2.3 \times 10^3$ cm^{-1}, $S_{max} = (\eta g_s S^*)_{max} = 2.3 \times 10^6$ cm^{-1}. Thus, value S in the case of parameter variation can increase by a thousand of times. If one turns now to the limits in which the characteristic bulk current density i^* can vary, it should be noted that exchange current i_0 in expression (18) also varies over a wide range at an increase in the temperature.

According to formula (2), if t_{ref} = 50°C, $i_0^{ref} = 10^{-8}$ A/cm^2, then at temperature t = 60°C $i_0 = 2.2 \times 10^{-8}$ A/cm^2, at t = 80°C $i_0 = 10^{-7}$ A/cm^2, and t = 95°C $i_0 = 2.8 \times 10^{-7}$ A/cm^2. Now, using formula (18) and estimates of S_{min} and S_{max}, one can find the values of the minimum and maximum values of the characteristic bulk current density. They are presented in Table 2.

Table 2 shows that we chose an active layer with a very high activity for performing calculations (the data of Fig. 2): characteristic bulk current density at t = 80°C $i^* = 1.04 \times 10^{-1}$ A/cm^3. This value is approximately two times lower than the maximum possible value presented in Table 2. Therefore, the values of overall current and power density turned out to be so high: at the potential of E = 0.6 V, overall current I = 4.57 A/cm^2 and power density W = 2.74 W/cm^2.

To show how the initial value of i^* (due to inevitable heating of the cathode active layer, the characteristic bulk current density increases) affects the overall characteristics of the cathode, we will proceed as follows. Let us perform the calculation of the overall characteristics of the cathode for three values of i^*, A/cm^3: 1.04×10^{-3}, 1.04×10^{-2}, 1.04×10^{-1}. The other parameters will remain the same as before: Δ = 3 μm, λ^* = 0.1 W/mC, δ = 400 μm, p^* = 505 kPa, I_d^* = 1.035 A/cm^2, α^* = 0.156. Let us consider a cathode with oxygen saturated by water vapors at t = 85°C in the bipolar plate channels. The calculation results are presented in Fig. 3 and Table 3.

At a decrease in i^*, the maximum value of the cathode density (Fig. 3b) decreases and its position is shifted towards lower potentials. As shown by the data in Table 3, if $i^* = 1.04 \times 10^{-1}$, then W_{max} = 2.74 W/cm^2 at E = 0.6 V; if $i^* = 1.04 \times 10^{-2}$, then W_{max} = 2.23 W/cm^2 at E = 0.5 V; and if $i^* = 1.04 \times 10^{-3}$, then W_{max} = 1.64 W/cm^2 at E = 0.4 V. The overall current values also become lower.

The chosen value of characteristic bulk current density $i^* = 1.04 \times 10^{-1}$ A/cm^3, as already stated, corresponds to the cathode active layer with a very high activity, which is also evidenced by the data in Table 2. As it is, at present, active layers with a much lower activity are used. Let us choose more moderate, more realistic characteristics for the parameters in formulas (18) and (19). Precisely, let us assume S^{**} = 30 m^2/g of Pt, ν = 0.6, g_w = 20 wt %, η = 50%. Then we obtain the value of the characteristic bulk current density $i^* = 1.39 \times 10^{-3}$ A/cm^3, the value that already practically coincides with the i^* value chosen for curves *1* of Fig. 3. In these curves, the overall characteristics, current I = 1.37 A/cm^2 and power density

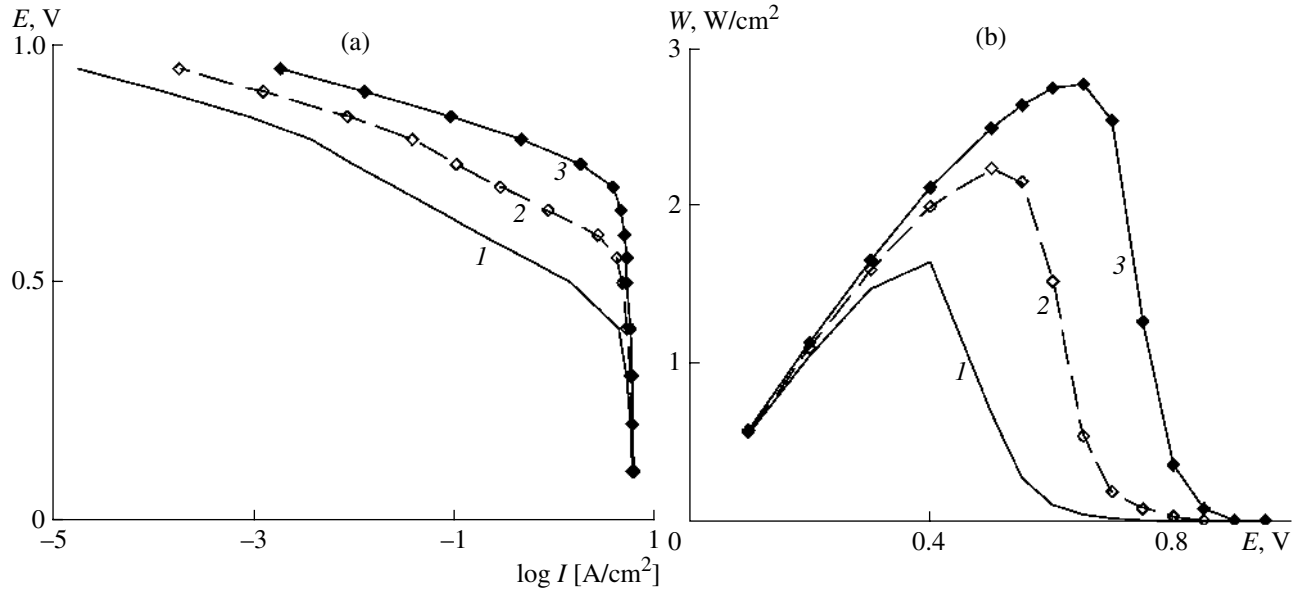

Fig. 3. (a) Tafel curves and (b) dependence of power density on the cathode potential. The working fuel cell temperature is 80°C, $\lambda^* = 0.1$ W/mC, $\delta = 400$ μm, $\Delta = 3$ μm, $p^* = 505$ kPa, oxygen is saturated by vapor at $t = 85$°C. i^*, A/cm^3: (*1*) 1.04×10^{-3}, (*2*) 1.04×10^{-2}, (*3*) 1.04×10^{-1}.

$W = 0.68$ W/cm^2, reach significant values only at the cathode potential $E = 0.5$ V. At the potential of $E = 0.6$ V, these values are extremely low: $I = 0.18$ A/cm^2 and $W = 0.11$ W/cm^2, which is graphically shown in Fig. 3b.

Large effect on the overall characteristics of the cathode with Nafion and platinum is produced by the active layer thickness. As shown in [18], high overall characteristics of the cathode can be reached by decreasing the active layer thickness to the values achieving units of micrometers. This trend is well illustrated by the data presented in Fig. 4. The cathodes operated at the fuel cell temperature of 80°C. The other parameters remained the same as before: $i^* = 1.04 \times 10^{-1}$ A/cm^3, $\lambda^* = 0.1$ W/mK, oxygen is saturated by vapor at $t = 85$°C, $p^* = 505$ kPa. The active layer thickness was 3, 10, and 30 μm.

At the potential of $E = 0.6$ V, the cathodes had the following parameters: overall current $I = 4.57$ A/cm^2, power density $W = 2.74$ W/cm^2 at $\Delta = 3$ μm; $I = 3.46$ A/cm^2, $W = 2.07$ W/cm^2 at $\Delta = 10$ μm; $I = 1.83$ A/cm^2, $W = 1.1$ W/cm^2 at $\Delta = 30$ μm. Simultaneously with a decrease in the overall current and power density at an increase in the active layer thickness, other overall characteristics also grow (Fig. 4b–4d): the active layer temperature, water vapor flow and reduced partial pressure of the vapor at the active layer surface adjacent to the gas–diffusion layer.

At the potential of $E = 0.6$ V, the following parameters were registered: active layer temperature $t^* = 129$°C, vapor flux (in the direction from the active layer to the bipolar plate) $I_w = 0.31$ A/cm^2, reduced partial pressure of the vapor at the active layer surface $p_{w1} = 0.51$ at $\Delta = 3$ μm; and $t^* = 118$°C, $I_w = 0.20$ A/cm^2, $p_{w1} = 0.37$ at $\Delta = 10$ μm; $t^* = 103$°C, $I_w = 0.08$ A/cm^2, $p_{w1} = 0.22$ at $\Delta = 30$ μm.

The last noteworthy cathode parameter is the effective thermal conductivity of the gas–diffusion layer λ^*. Smallness of this parameter can result in heating of the cathode active layer, due to which a possibility of significant increase in the overall current and cathode power density appears. The results of λ^* variation are presented in Fig. 5. Three values of λ^*, W/mC, were chosen: 0.1, 0.15, and 0.2. It is found that the overall currents and power density values (Fig. 5a) are little sensitive towards the variation in parameter λ^*. However, the active layer temperature (Fig. 5b) and the vapor flow value (Fig. 5c) vary significantly at the variation in λ^*, which was to be expected.

At the potential of $E = 0.6$ V, we have the following parameter values: active layer temperature $t^* = 129$°C, vapor flow $I_w = 0.31$ A/cm^2, reduced partial pressure of the vapor at the active layer surface $p_{w1} = 0.51$ at $\lambda^* = 0.1$ W/mK; and $t^* = 114$°C, $I_w = 0.13$ A/cm^2, $p_{w1} = 0.32$ at $\lambda^* = 0.15$ W/mK; $t^* = 106$°C, $I_w = 0.06$ A/cm^2, $p_{w1} = 0.25$ at $\lambda^* = 0.2$ W/mK. Thus, variation of the value of effective thermal conductivity of the gas–diffusion layer can also be used for searching the optimum value of the vapor flow, the value that provides optimum Nafion humidification in the fuel cell cathode.

CONCLUSION

Computer simulation of the principal processes occurring on the cathode of the fuel cell with Nafion as electrolyte and with a platinum catalyst is carried out. The following processes are considered: current generation in the active layer; heat exchange consisting in the equilibrium dissipation of heat evolved in the cathode

Table 3. Dependence of the overall characteristics of the oxygen cathode on the characteristic bulk current density value (fuel cell working temperature $t = 80°C$, $\Delta = 3$ μm, $\lambda^* = 0.1$ W/mK, $\delta = 400$ μm, $p^* = 505$ kPa, $I_d^* = 1.035$ A/cm^2, $\alpha^* = 0.156$, oxygen in the bipolar plate is saturated by water vapor at $t = 85°C$)

i^*, A/cm^3	E, V	I, A/cm^2	W, W/cm^2
1.04×10^{-1}	0.8	0.44	0.36
	0.7	3.62	2.53
	0.6	4.57	2.74
	0.5	4.97	2.48
	0.4	5.27	2.11
	0.3	5.49	1.65
1.04×10^{-2}	0.8	0.04	0.03
	0.7	0.27	0.19
	0.6	2.52	1.51
	0.5	4.46	2.23
	0.4	4.98	1.99
	0.3	5.28	1.59
1.04×10^{-3}	0.8	3.6×10^{-3}	2.9×10^{-3}
	0.7	0.03	0.02
	0.6	0.18	0.11
	0.5	1.37	0.68
	0.4	4.10	1.64
	0.3	4.91	1.49

active layer through the gas-diffusion layer into the bipolar plate; gas exchange in the gas–diffusion layer: supply of oxygen to the active layer and the corresponding attainment of the limiting current on the cathode; vapor exchange in the gas–diffusion layer affecting the humidification degree of Nafion in the fuel cell; oxygen (air) saturation by water vapor in the bipolar plate channels, its effect on the value of the current on the cathode.

It is shown how the unavoidable heating of the cathode active layer results in an increase in the current significantly enhancing the value of overall characteristics of the cathode (current and power density).

It is found that the conventional choice of the temperature of the saturated water vapor in the bipolar plate channels (by 5°C higher than the fuel cell temperature) does not result in enhancement in the water vapor supply towards the Nafion membrane, but only assists the decrease in the value of the vapor flow from the active layer to the bipolar plate. This eventually leads to optimization of Nafion humidification in the fuel cell.

The effect of the values of the principal parameters characterizing the operation of the cathode with Nafion and platinum is studied: the characteristic bulk current density in the range of high potentials, active layer thickness and effective thermal conductivity of the gas–diffusion layer and their influence on the overall current on the cathode is shown.

APPENDIX

Designations of parameters characterizing the active and gas–diffusion layers of the cathode with Nafion and platinum and also with the gas reagent in the bipolar plate channels and designations used in their calculations

ACTIVE LAYER

External parameters

$t = 80°C$ is the fuel cell external temperature

$p^* = 101$ and 505 kPa are the values of the vapor–gas mixture pressure in the bipolar plate channels

Δ, μm = 3, 10, 30 are the active layer thickness values

$\eta = 60\%$ is the performance of the cathode

Parameters of the electrochemical kinetics of the process of oxygen reduction on platinum

$E_{st} = 1.05$ V is the steady–state potential of the cathode

$E^* = 0.825$ V is the potential of the break point on the Tafel curve

$b_1 = (6 \times 10^{-2}/2.3)$ V $= 2.6 \times 10^{-2}$ V is the Tafel curve slope in the range of high potentials

$b_2 = (12 \times 10^{-2}/2.3)$ V $= 5.2 \times 10^{-2}$ V is the Tafel curve slope in the range of low potentials

$n = 4$ is the amount of electrons participating in the electrochemical process

$F = 9.6 \times 10^4$ C/mol is the Faraday number

i_0, A/cm^2 is the exchange current in the range of high potentials

i^*, A/cm^3 $= 1.04 \times 10^{-3}$, 1.04×10^{-2}, 1.04×10^{-1} are the characteristic bulk current densities in the range of high potentials

Parameters of the active layer optimum structure

$g_e = 0.475$ is the bulk concentration of Nafion grains

$g_s = 0.525$ is the bulk concentration of the support grains

$g_0 = 0$ is the bulk concentration of cavity grains

g_w is the mass content of platinum in the support grains

S, cm^{-1} is the catalyst (platinum) specific surface area

S^{**}, m^2/g Pt is the catalyst (platinum) specific surface area

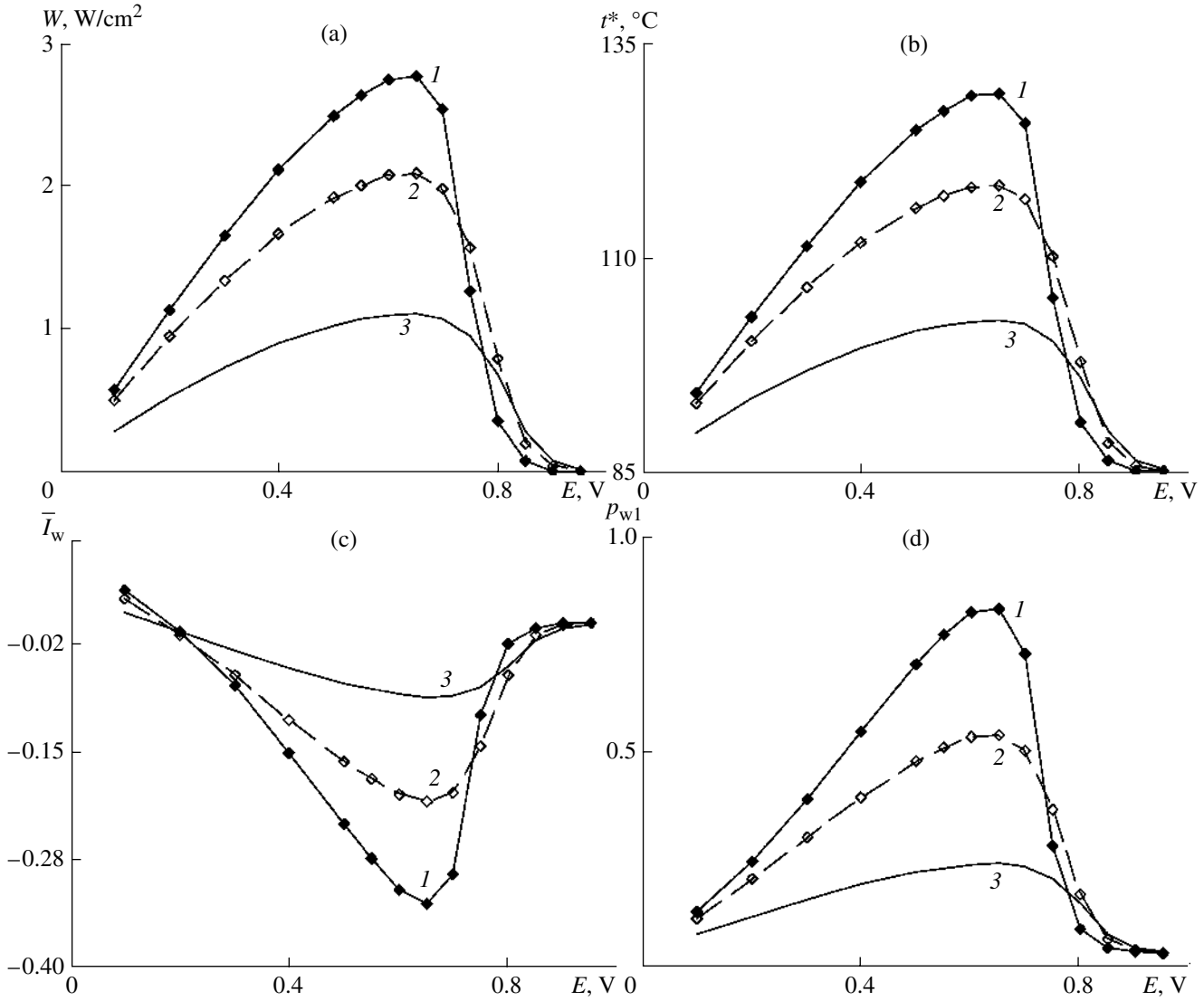

Fig. 4. Dependences on the cathode potential of: (a) power density, (b) active layer temperature, (c) reduced water vapor flow, (d) reduced partial oxygen pressure at the interface of the active and gas–diffusion layer. The working fuel cell temperature is 80°C, $i^* = 1.04 \times 10^{-1}$ A/cm^3, $\lambda^* = 0.1$ W/mC, $\delta = 400$ μm, $p^* = 505$ kPa, oxygen is saturated by vapor at $t = 85$°C. Δ, μm: (*1*) 3, (*2*) 10, (*3*) 30.

$d_s = 30$ nm is the average diameter of pores in the support grains

η is the fraction of the catalyst active surface

$\nu = 0.5$ is the porosity of support grains

$\rho_p = 21.5$ g/cm^3 is the catalyst (platinum) density

$\rho_c = 1.8$ g/cm^3 is the support (carbon black) density

Parameters determining the processes of mass and electric transfer

$D^* = 5.49 \times 10^{-4}$ cm^2/s is the effective diffusion coefficient of oxygen in the active layer

$D_{kn} = 4 \times 10^{-3}$ cm^2/s is the Knudsen diffusion coefficient of oxygen in the support grain pores

$c_0 = 5 \times 10^{-6}$ and 2.5×10^{-5} g-mol/cm^3 is the oxygen solubility in Nafion at $p^* = 101$ and 505 kPa

$k^* = 8.37 \times 10^{-3}$ Ohm^{-1} cm^{-1} is the effective specific conductivity of Nafion at optimum humidification

$k = 1 \times 10^{-1}$ Ohm^{-1} cm^{-1} is the specific conductivity of Nafion at optimum humidification

$\bar{I} = I/I_d$ is the reduced overall current generated in the active cathode layer

GAS–DIFFUSION LAYER

p_s is the reduced partial pressure of oxygen at the interface of the active and gas–diffusion layers

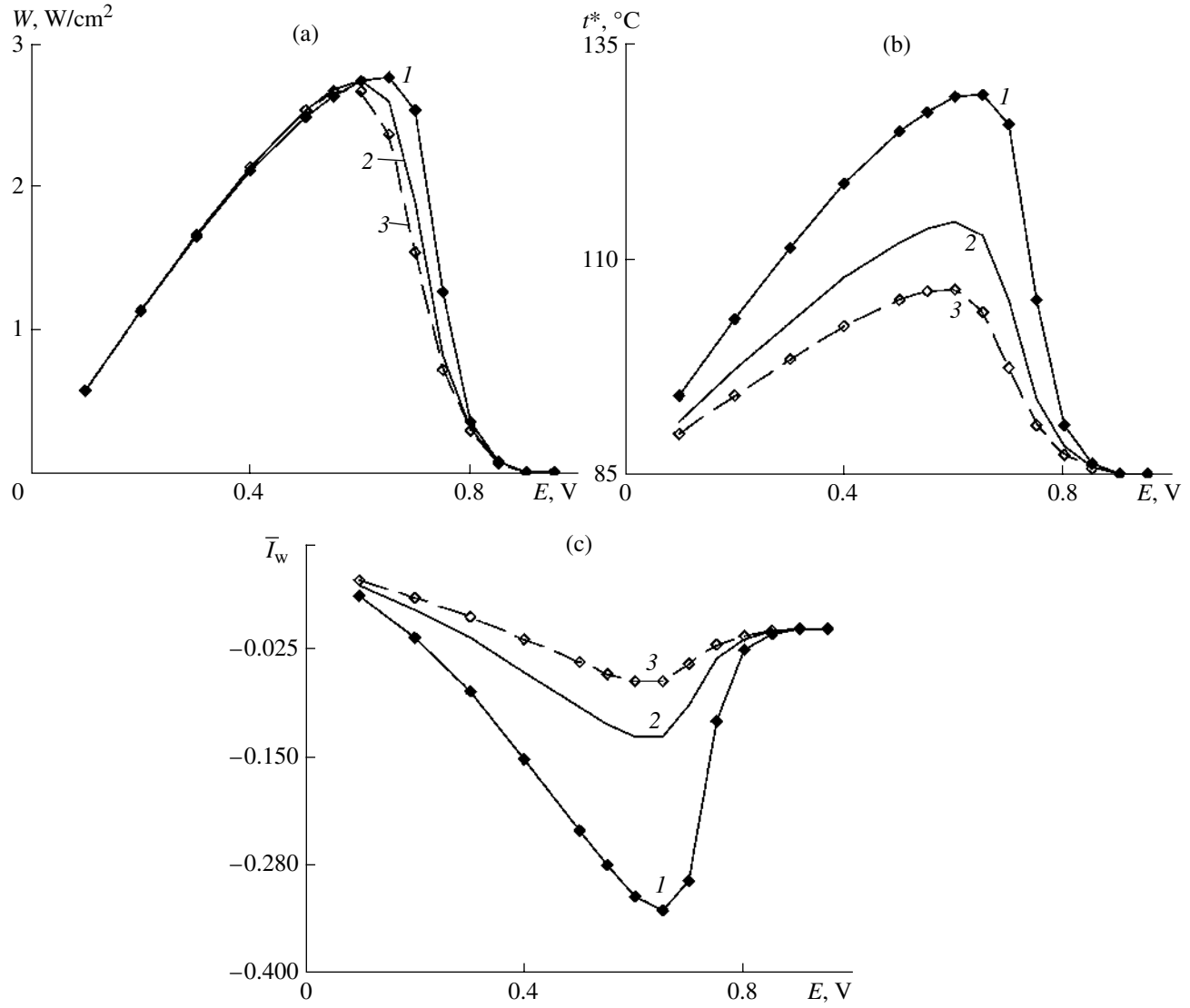

Fig. 5. Dependences on the cathode potential of: (a) power density, (b) active layer temperature, (c) reduced water vapor flow. The working fuel cell temperature is 80°C, $i^* = 1.04 \times 10^{-1}$ A/cm^3, $\Delta = 3$ μm, $\delta = 400$ μm, $p^* = 505$ kPa, oxygen is saturated by vapor at $t = 85$°C. λ*, W/mC: (*1*) 0.1, (*2*) 0.15, (*3*) 0.2.

p_n is the reduced partial pressure of nitrogen at the interface of the active and gas–diffusion layers

p_{w1} is the reduced partial pressure of water vapors at the interface of the active and gas–diffusion layers

D^{**} is the effective diffusion coefficient of the gas vapor mixture

u^* is the characteristic rate of has–vapor mixture movement

$I_d = I_d^* \varepsilon$ is the diffusion current in the gas–diffusion layer

$I_d^* = 1.035$ A/cm^2 is the characteristic diffusion current in the gas–diffusion layer

$\varepsilon = p^*/p_0^*$, $p_0^* = 101$ kPa

$\alpha = \alpha^* \varepsilon$ is the ratio of the characteristic rate of the vapor–gas mixture filtration to its diffusion rate

$\alpha^* = 0.156$

$\overline{I_w} = nFI_w/I_d$ is the reduced water vapor flow in the gas–diffusion layer

λ*, W/mC = 0.1, 0.15, 0.2 is the effective thermal conductivity of the gas–diffusion layer

$\delta = 400$ μm is the thickness of the gas–diffusion layer

GAS REAGENT IN THE BIPOLAR PLATE CHANNELS

p_0 is the reduced partial pressure of oxygen in the bipolar plate channels

p_{N0} is the reduced partial pressure of nitrogen in the bipolar plate channels

p_{w0} is the reduced partial pressure of water vapors in the bipolar plate channels

t, °C = 85, 95 is the temperature of saturated water vapor in the bipolar plate channels

REFERENCES

1. Parthasarathy, A., Srinivasan, S., Appleby, A.J., and Martin, C.R., *J. Electrochem. Soc.*, 1992, vol. 139, p. 2530.
2. Mitsushima, S., Araki, N., Kamiya, N., and Ota, K., *J. Electrochem. Soc.*, 2002, vol. 149, p. A1371.
3. Ju, H., Meng, H., and Wang, C-Y., *Int. J. Heat Mass Transfer*, 2005, vol. 48, p. 1303.
4. Ramousse, J., Deseure, J., Lottin, O., Didierjean, S., and Maillet, D., *J. Power Sources*, 2005, vol. 145, p. 416.
5. Khandelwal, M. and Mench, M.M., *J. Power Sources*, 2006, vol. 161, p. 1106.
6. Chirkov, Yu.G. and Rostokin, V.I., *Elektrokhimiya*, 2007, vol. 43, p. 25 [*Russ. J. Elektrochem.* (Engl. Transl.), vol. 43, p. 25].
7. Chirkov, Yu.G. and Rostokin, V.I., *Elektrokhimiya*, 2008, vol. 44, p. 981 [*Russ. J. Elektrochem.* (Engl. Transl.), vol. 44, p. 910].
8. Chirkov, Yu.G. and Rostokin, V.I., *Elektrokhimiya*, 2006, vol. 42, p. 806 [*Russ. J. Elektrochem.* (Engl. Transl.), vol. 42, p. 715].
9. Vie, J.S.P. and Kjelstrup, S., *Electrochim. Acta*, 2004, vol. 49, p. 1069.
10. Shimpalee, S., Beuscher, U., and Van Zee, J.W., *Electrochim. Acta*, 2007, vol. 52, p. 6748.
11. Ramousse, J., Didierjean, S., Lottin, O., and Maillet, D., *Intern. J. Thermal Sciences*, 2008, vol. 47, p. 1.
12. Costamagna, P. and Srinivasan, S., *J. Power Sources*, 2001, vol. 102, p. 253.
13. Ticianelli, E.A., Derouin, C.R., Redondo, A., and Srinivasan, S., *J. Electrochem. Soc.*, 1998, vol. 135, p. 2209.
14. Ralph, T.R., Hards, G.A., Keating, J.E., Campbell, S.A., Wilkinson, D.P., Davis, M., St-Pierre, J., and Johnson, M.C., *J. Electrochem. Soc.*, 1997, vol. 144, p. 3845.
15. Kocha, S.S, in *Handbook of Fuel Cells - Fundamentals, Technology and Applications. Vol. 3. Ch. 43*, Vielstich, W., Lamm, A., and Gasteiger, H., Eds., Chichester,: UK: Wiley, 2003, p. 538.
16. Gasteiger, H, Gu, W, Makharia, R, Mathias, M.F, and Sompalli, B, in *Handbook of Fuel Cells – Fundamentals, Technology and Applications. Vol. 3. Ch. 46*, Vielstich, W., Lamm, A.., and Gasteiger, H., Eds., Chichester, UK: Wiley, 2003, p. 593.
17. Chirkov, Yu.G. and Rostokin, V.I., *Elektrokhimiya*, 2006, vol. 42, p. 799 [*Russ. J. Elektrochem.* (Engl. Transl.), vol. 42, p. 722].
18. Chirkov, Yu.G. and Rostokin, V.I., *Elektrokhimiya,* 2007, vol. 43, p. 827 [*Russ. J. Elektrochem.* (Engl. Transl.), vol. 43, p. 787].

SPELL: 1. ok